mer-$[Mn(CO)_3(CNC_6H_5)_3]^+$, 70877-80-4; fac-$[Mn(CO)_3(CNC_6H_5)_3]^+$, 70800-84-9; cis-$[Mn(CO)_4(CNC_6H_5)_2]^+$, 70800-82-7; trans-$[Mn(CO)_4(CNC_6H_5)_2]^+$, 80695-81-4; $[Mn(CO)_5(CNC_6H_5)]^+$, 80642-45-1; $Cr(CNCH_3)_6$, 80642-46-2; $Cr(CO)(CNCH_3)_5$, 80658-41-9; trans-$[Cr(CO)_2(CNCH_3)_4]$, 80696-55-5; cis-$[Cr(CO)_2(CNCH_3)_4]$, 80642-47-3; mer-$[Cr(CO)_3(CNCH_3)_3]$, 80695-82-5; fac-$[Cr(CO)_3(CNCH_3)_3]$, 80695-83-6; cis-$[Cr(CO)_4(CNCH_3)_2]$, 37131-11-6; trans-$[Cr(CO)_4(CNCH_3)_2]$, 80695-84-7; $Cr(CO)_5(CNCH_3)$, 33726-04-4; $Cr(CO)_6$, 13007-92-6; $Cr(CNC_5H_6)_6$, 17375-15-4; $Cr(CO)(CNC_5H_6)_5$, 70800-89-4; trans-$[Cr(CO)_2(CNC_5H_6)_4]$, 80695-85-8; cis-$[Cr(CO)_2(CNC_5H_6)_4]$, 70800-88-3; mer-$[Cr(CO)_3(CNC_5H_6)_3]$, 80695-86-9; fac-$[Cr(CO)_3(CNC_5H_6)_3]$, 70831-80-0; cis-$[Cr(CO)_4(CNC_5H_6)]$, 70831-79-7; trans-$[Cr(CO)_4(CNC_5H_6)_2]$, 80695-87-0; $Cr(CO)_5(CNC_5H_6)$, 14782-94-6.

Direct Determination of Rate Constants of Slow Dynamic Processes by Two-Dimensional "Accordion" Spectroscopy in Nuclear Magnetic Resonance

Geoffrey Bodenhausen and R. R. Ernst*

Contribution from the Laboratorium für Physikalische Chemie, Eidgenössische Technische Hochschule, 8092 Zürich, Switzerland. *Received August 18, 1981*

Abstract: A novel class of NMR experiments, based on the systematic variation of three time variables, permits both the identification of exchange networks and the direct measurement of the corresponding rate constants. Linear combinations of cross sections taken from two-dimensional spectra allow a straightforward analysis of nonexponential recovery behavior by identifying normal modes. The line widths of the resulting Lorentzian line shapes provide a direct measure of the rate constants of various dynamic processes, such as chemical exchange, transient Overhauser effects, and spin-lattice relaxation.

I. Introduction

The study of slow dynamic processes by nuclear magnetic resonance is of practical importance in numerous applications, including transient nuclear Overhauser effects[1-3] and polarization transfer associated with slow chemical exchange.[4] Both processes lead to very similar phenomena in NMR spectroscopy and can be studied by the same experimental techniques.

Nuclear Overhauser effects have proven to be of extraordinary importance for the determination of molecular structure of biomolecules in solution.[5-10] In particular, these effects allow the elucidation of amino acid sequences and tertiary structures in proteins.

The study of chemical processes by NMR has long been known to provide unique insight into molecular dynamics.[11,12] A particular virtue lies in the ability to study dynamic equilibria without the need for chemical perturbations. Very fast reactions can be studied through their effect on nuclear relaxation, since they contribute to the spectral densities at the Larmor frequency.[13] An intermediate regime, with reaction rates comparable to chemical shift differences, to spin couplings or quadrupolar splittings, can be studied by line-shape analysis.[12,14] Slow exchange processes, with rates smaller than typical line widths, may be characterized by monitoring the transfer of nuclear polarization between inequivalent sites. In selective magnetization transfer experiments,[4] the longitudinal magnetization of a specific site is labeled by selective saturation or inversion. The exchange process can be traced out by monitoring the migration of the nonequilibrium magnetization to other sites. This migration occurs in a mixing interval t_m which separates the initial perturbation and the observation by a nonselective pulse.

It has recently been shown that magnetization transfer experiments can be carried out much more efficiently by two-dimensional spectroscopy,[15] both for NOE studies of biomolecules[16-20] and for the investigation of chemical exchange.[21,22] All sites are labeled in a single experiment without previous knowledge of the spectrum, thus allowing all exchange pathways to be observed simultaneously. Thus the 2-D method greatly enhances the information obtained per unit of time. In addition, problems associated with selective irradiation in crowded spectra are completely avoided.

For a quantitative measurement of the exchange rates, it is normally not sufficient to record one 2-D spectrum with a single mixing time, t_m. Often, it is necessary to observe the magnetization transfer as a function of the mixing time by obtaining a set of 2-D spectra for different t_m delays. The recording of the buildup and decay of the transfer represents, in effect, an extension from

(1) Solomon, I. *Phys. Rev.* **1955**, *99*, 559.
(2) Abragam, A. "Principles of Nuclear Magnetism"; Oxford University Press, 1960; p 333.
(3) Noggle, J. S.; Schirmer, R. E. "The Nuclear Overhauser Effect. Chemical Applications"; Academic Press: New York, 1971.
(4) Forsen, S. H.; Hoffman, R. A. *J. Chem. Phys.* **1963**, *39*, 2892; **1964**, *40*, 1189; **1966**, *45*, 2049.
(5) Campbell, I. D.; Dobson, C. M.; Williams, R. J. P. *J. Chem. Soc., Chem. Commun.* **1974**, 888.
(6) Hull, W. E.; Sykes, B. D. *J. Chem. Phys.* **1975**, *63*, 867.
(7) Kalk, A.; Berendsen, H. J. C. *J. Magn. Reson.* **1976**, *24*, 343.
(8) Gordon, S. L.; Wüthrich, K. *J. Am. Chem. Soc.* **1978**, *100*, 7094.
(9) Richarz, R.; Wüthrich, K. *J. Magn. Reson.* **1978**, *30*, 147.
(10) Wagner, G.; Wüthrich, K. *J. Magn. Reson.* **1979**, *33*, 675.
(11) Gutowsky, H. S.; McCall, D. M.; Slichter, C. P. *J. Chem. Phys.* **1953**, *21*, 279. Gutowsky, H. S.; Saika, A. *Ibid.* **1953**, *21*, 1688.
(12) "Dynamic NMR Spectroscopy"; Jackman, L. M.; Cotton, F. A., Ed.; Academic Press: New York, 1975.
(13) Laszlo, P. *Prog. Nucl. Magn. Reson. Spectrosc.* **1980**, *13*, 257.
(14) Binsch, G. *J. Am. Chem. Soc.* **1969**, *91*, 1304.
(15) Jeener, J.; Meier, B. H.; Bachmann, P.; Ernst, R. R. *J. Chem. Phys.* **1979**, *71*, 4546.
(16) Macura, S.; Ernst, R. R. *Mol. Phys.* **1980**, *41*, 95.
(17) Kumar, Anil; Ernst, R. R.; Wüthrich, K. *Biochem. Biophys. Res. Commun.* **1980**, *95*, 1.
(18) Kumar, Anil; Wagner, G.; Ernst, R. R.; Wüthrich, K. *Biochem. Biophys. Res. Commun.* **1980**, *96*, 1156.
(19) Bösch, C.; Kumar, Anil; Baumann, R.; Ernst, R. R.; Wüthrich, K. *J. Magn. Reson.* **1981**, *42*, 159.
(20) Kumar, Anil; Wagner, G.; Ernst, R. R.; Wüthrich, K. *J. Am. Chem. Soc.* **1981**, *103*, 3654.
(21) Meier, B. H.; Ernst, R. R. *J. Am. Chem. Soc.* **1979**, *101*, 6441.
(22) Huang, Y.; Macura, S.; Ernst, R. R. *J. Am. Chem. Soc.*, **1981**, *103*, 5327.

0002-7863/82/1504-1304$01.25/0

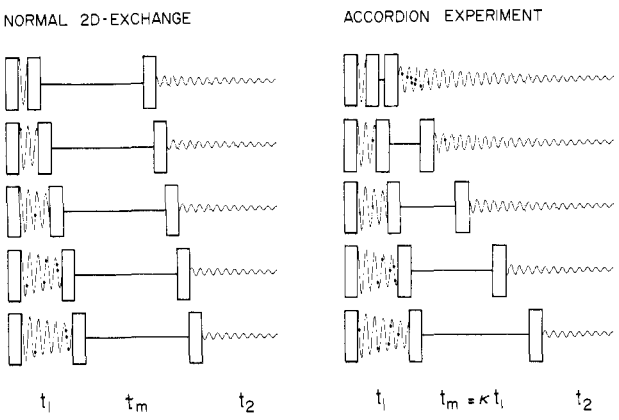

Figure 1. Schematic representation of the pulse sequences used for normal 2-D exchange spectroscopy (left) and for the accordion experiment (right). Both sequences employ three 90° pulses, separated by the evolution time (t_1) and the mixing time (t_m) and followed by the detection time (t_2). In contrast to the normal experiment, where t_m is kept constant for all t_1 increments, the accordion method employs a variable mixing time t_m which is stepped together with t_1. In both experiments, the phase of the first pulse is alternated with corresponding addition and subtraction of the signals.

two- to three-dimensional NMR. Although conceptually straightforward, this extension tends to put prohibitive demands on experimental time.

In this paper, a novel approach, which will be referred to as "accordion spectroscopy", is proposed in order to reduce the dimension from three to two. Apart from a significant time saving, the exchange rates are presented in a novel and simple form.

After a brief review of the 2-D exchange method in section II, the basic idea of accordion spectroscopy is introduced in section III. Experimental results for the ring inversion of *cis*-decalin are presented in section IV, which is followed by a section describing various strategies for interpretation. Finally, section VI briefly discusses extensions to more complex networks. Section VII deals with coupled spins, and the relation to true three-dimensional spectroscopy is discussed in the Conclusion.

II. Two-Dimensional Exchange Spectroscopy

Before introducing the accordion experiment, a brief review of 2-D exchange spectroscopy appears in order. More detailed accounts can be found elsewhere.[15,16] For simplicity, the treatment will be restricted to a two-site exchange case with equal populations and with equal spin–lattice relaxation times. In addition, we shall focus attention on proton-decoupled carbon-13 spectroscopy, where a purely classical description of transverse and longitudinal magnetization is appropriate. In particular, complications due to multiple-quantum effects (which arise in coupled proton systems and lead to so-called J cross-peaks[23]) can be excluded by considering only isolated $I = {}^1/_2$ spins.

The basic 2-D exchange experiment[15] employs a simple sequence of three 90° pulses as shown in Figure 1. Instead of the selective 180° inversion pulse used in magnetization transfer experiments, a pair of nonselective 90° pulses, separated by an evolution period t_1, is employed to frequency-label the magnetization. If we consider two sites A and B with distinct chemical shifts Ω_A and Ω_B, the transverse magnetization vectors generated by the first $90°_x$ pulse will precess in the evolution period t_1 (neglecting transverse relaxation and exchange)

$$M_y^A(t_1) = -M_0^A \cos \Omega_A t_1 \quad (1)$$

$$M_y^B(t_1) = -M_0^B \cos \Omega_B t_1 \quad (2)$$

with the equilibrium magnetizations M_0^A and M_0^B. The second $90°_x$ pulse tips the y components back along the z axis, thereby setting up frequency-labeled populations:

$$M_z^A(t_1) = -M_0^A \cos \Omega_A t_1 \quad (3)$$

$$M_z^B(t_1) = -M_0^B \cos \Omega_B t_1 \quad (4)$$

Dynamic processes such as cross-relaxation or slow chemical exchange (characterized by a first order rate constant k) may interconvert magnetization M_z^A and M_z^B during the mixing interval t_m. At the same time, the spin–lattice relaxation rate R_1 will tend to attenuate the memory of the initial labeling:

$$M_z^A(t_1,t_m) = -{}^1/_2 M_0^A[(1 + e^{-2kt_m}) \cos \Omega_A t_1 + (1 - e^{-2kt_m}) \cos \Omega_B t_1] e^{-R_1 t_m} \quad (5)$$

$$M_z^B(t_1,t_m) = -{}^1/_2 M_0^B[(1 - e^{-2kt_m}) \cos \Omega_A t_1 + (1 + e^{-2kt_m}) \cos \Omega_B t_1] e^{-R_1 t_m} \quad (6)$$

More general expressions can be found elsewhere.[16]

After the final 90° pulse in Figure 1, two transverse magnetization vectors with frequencies Ω_A and Ω_B can be detected as a function of the time variable t_2. Their amplitudes (and thus the intensities of the Lorentzian lines after Fourier transformation with respect to t_2) are directly proportional to the polarizations expressed by eq 5 and 6. These signals are recorded for regular increments of t_1. By another Fourier transformation with respect to t_1, different pathways of the magnetization can be unraveled. For instance, magnetization which has precessed at Ω_A in t_1 and resumes precession at Ω_B after mixing will appear as a cross-peak at $\omega_1 = \Omega_A$ and $\omega_2 = \Omega_B$. Diagonal peaks, also referred to as auto-peaks, reflect magnetization which has failed to migrate from one site to another ($\omega_1 = \omega_2 = \Omega_A$ or $\omega_1 = \omega_2 = \Omega_B$). The amplitudes of the peaks in the 2-D spectrum are determined by the t_1-independent mixing coefficients found in eq 5 and 6:

$$a_{AA}(t_m) = a_{BB}(t_m) = {}^1/_2[1 + e^{-2kt_m}] e^{-R_1 t_m} \quad (7)$$

$$a_{AB}(t_m) = a_{BA}(t_m) = {}^1/_2[1 - e^{-2kt_m}] e^{-R_1 t_m} \quad (8)$$

where a_{AA} and a_{BB} are responsible for the diagonal peaks and a_{AB} and a_{BA} for the cross-peaks. The amplitudes are actually governed by the same laws that determine signal intensities in selective magnetization transfer experiments.

Note that the very appearance of a cross-peak is sufficient proof that exchange is taking place between sites A and B. For a qualitative analysis of the exchange pathways, a single exchange spectrum is sufficient. Examples of such investigations have been described earlier for cross-relaxation[16-20] and for chemical exchange networks.[21,22]

Of great practical concern is an efficient strategy for a quantitative determination of the exchange rates. In the simple situation of a two-site exchange system with equal populations and equal relaxation rates, represented by eq 7 and 8, the exchange rate k can be determined directly from the ratio of cross- and auto-peak intensities, which is independent of the relaxation rate R_1:

$$\frac{a_{AA}}{a_{AB}} = \frac{1 + e^{-2kt_m}}{1 - e^{-2kt_m}} \simeq \frac{1 - kt_m}{kt_m} \quad (9)$$

The latter equation holds within the limitations of the initial rate approximation.

In many situations the evaluation of eq 9 is not feasible for at least two reasons. First, the auto-peaks a_{AA} and a_{BB} are often hidden in an ill-resolved "ridge" along the main diagonal, and their amplitudes cannot be measured accurately. This is typical for 2-D NOE spectra of proteins[17-20] where it is difficult to identify individual resonances along the main diagonal, although the cross-peaks may be quite well resolved. In such situations, the analysis must therefore be based on the cross-peaks alone. Second, in most systems of practical interest, several exchange mechanisms or cross-relaxation pathways concur to form extensive networks, and it is no longer possible to derive exchange rates from simple ratios as in eq 9.

For these reasons, it is often necessary to record a series of 2-D exchange spectra with different t_m values.[20] Numerical evaluation of the t_m dependence of the cross-peak intensities yields a quan-

(23) Macura, S.; Huang, Y.; Suter, D.; Ernst, R. R. *J. Magn. Reson.* **1981**, *43*, 259.

titative measure of the rate constants involved. This procedure requires a true three-dimensional data set to be recorded as a function of three time variables, t_1, t_m, and t_2. Obviously, an experiment of this kind can be exceedingly time consuming and will become prohibitive if the temperature dependence of the exchange process must be determined as well. Furthermore, the comparison of peak amplitudes among a series of 2-D spectra may be fraught with danger if instrumental instabilities affect absolute intensities.

III. Accordion Spectroscopy

In order to reduce the time requirements of a true three-dimensional experiment with three time variables, t_1, t_m, and t_2, we propose to increment two variables simultaneously by defining

$$t_m = \kappa t_1 \tag{10}$$

This proportionality is the central feature of the novel experiment. The coupling of t_m and t_1 in effect reduces a 3-D experiment to a special form of a 2-D experiment, with the usual independent variables t_1 and t_2. The pulse sequences appropriate for normal 2-D exchange spectroscopy and for accordion spectroscopy are shown schematically in Figure 1. The concerted stretching of evolution and mixing times recalls the motion of an accordion.

The three-dimensional information is now contained in a 2-D data set. A Fourier transformation with respect to t_1 is at the same time a Fourier transformation with respect to t_m. In the corresponding frequency domain, the ω_1 and ω_m axes run in parallel, but the spectral width spanned in ω_m differs by the factor κ from the spectral width in ω_1.

In accordion exchange spectroscopy, the meaning of the ω_1 and ω_m variables is quite different. The evolution during t_1 leads to narrow resonance lines with positions that characterize the original sites of the migrating magnetization. The *peak positions* along the ω_1/ω_m axis therefore must be referred to the ω_1 frequency variable. The exchange process during the mixing time t_m causes a slow variation of the signal amplitudes and is responsible for the *line shapes* along the ω_1/ω_m axis, which must be measured in units of the ω_m frequency variable. The scaling parameter κ is typically chosen between 10 and 100, depending on the exchange rates and the resolution of the spectrum under investigation. (Large κ factors cause broad lines which may interfere in spectra with closely spaced chemical shifts.)

The line shape resulting from the magnetization-exchange process during t_m can be calculated by Fourier transformation of eq 7 and 8:

$$S_{AA}(\omega_m) = S_{BB}(\omega_m) = \frac{1}{2}\left[\frac{R_1}{R_1^2 + \omega_m^2} + \frac{2k + R_1}{(2k + R_1)^2 + \omega_m^2}\right] \tag{11}$$

$$S_{AB}(\omega_m) = S_{BA}(\omega_m) = \frac{1}{2}\left[\frac{R_1}{R_1^2 + \omega_m^2} - \frac{2k + R_1}{(2k + R_1)^2 + \omega_m^2}\right] \tag{12}$$

These expressions refer to cross sections extracted from the two-dimensional spectrum parallel to the ω_m axis. They apply to absorption-mode phase-sensitive spectra. The frequency origin ($\omega_m = 0$) for each line-shape function is centered at the chemical shift (Ω_A or Ω_B) in the ω_1 domain.

Theoretical line shapes corresponding to eq 11 and 12 are shown in Figure 2. According to eq 11, the diagonal peaks consist of a *sum* of two Lorentzians with equal integrated intensities but different widths. The cross-peaks, on the other hand (eq 12), have line shapes determined by the *difference* of the same two Lorentzians. The integral of $S_{AB}(\omega_m)$ vanishes, which is consistent with the fact that no exchange can occur in a vanishing mixing time, i.e., for $t_m = 0$.

So far, it has been assumed that the line shapes are due exclusively to spin–lattice relaxation and exchange in t_m. In actual fact, transverse relaxation and inhomogeneous broadening during the evolution period t_1, expressed by the effective relaxation rate

Figure 2. Simulated accordion line shapes for diagonal peaks (top) and cross-peaks (below) for a symmetrical two-site exchange case. The time-domain signals (left) show oscillating components cos $\Omega_A t_1$ with envelopes $a_{AA}(t_m)$ (top left) and $a_{AB}(t_m)$ (bottom left), described by eq 7 and 8. The Fourier transforms reveal characteristic line shapes in the new ω_m domain. The diagonal peak $S_{AA}(\omega_m)$ (top right) consists of the sum of two Lorentzians with line widths R_1 and $2k + R_1$ (eq 11), while the cross-peak $S_{AB}(\omega_m)$ (bottom right) is composed of the difference of the same pair of Lorentzians according to eq 12. In these illustrations, $2k + R_1 = 3R_1$.

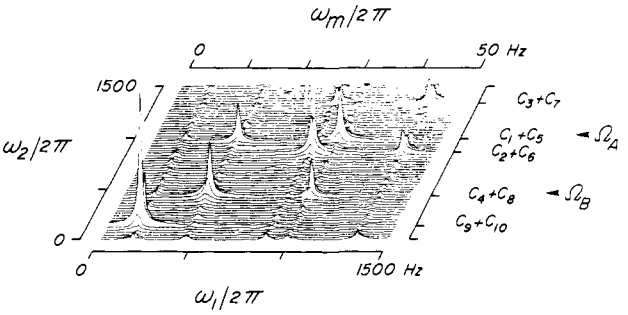

Figure 3. Proton-decoupled carbon-13 accordion spectrum of *cis*-decalin (I). Five distinct chemical shifts correspond to pairs of inequivalent sites as indicated. Exchanging signals $C_4 + C_8 \rightleftarrows C_1 + C_5$ and $C_2 + C_6 \rightleftarrows C_3 + C_7$ give rise to off-diagonal cross-peaks. The spectral width covers 1500 Hz in both ω_1 and ω_2 domains but only 50 Hz in the ω_m dimension ($\kappa = 30$). The spectrum was recorded at 240 K on a Bruker CXP 300 spectrometer. The array of 512 × 256 data points was zero-filled to 1024 × 512. In this absolute-value display mode, the characteristic line shapes are obscured. Ω_A and Ω_B indicate the ω_2 coordinates of the cross sections shown in Figures 4–6.

R_2^*, may also contribute. This leads to an additional damping of the magnetization given by eq 7 and 8 and to a broadening of the line shapes in the ω_m frequency domain. Because the line widths are expressed in ω_m units, a scaling factor κ must be taken into consideration. The line shapes (eq 11 and 12) must be modified by substitution of $R_1 + R_2^*/\kappa$ instead of R_1.

IV. Experimental Example: *cis*-Decalin

The ring inversion of *cis*-decalin (I) represents a typical case of two-site chemical exchange with equal populations that is suitable to demonstrate the features of accordion spectroscopy.

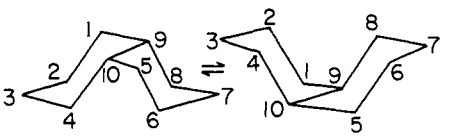

I

It has been investigated previously by 2-D exchange spectroscopy[22] as well as by conventional exchange methods.[24-26] There are five pairs of inequivalent carbon nuclei. The resonance at $C_9 + C_{10}$ is invariant to ring inversion while four pairs of sites interchange their chemical shifts: $C_1 \rightleftarrows C_4$, $C_2 \rightleftarrows C_3$, $C_5 \rightleftarrows C_8$, and $C_6 \rightleftarrows C_7$.

(24) Jensen, F. R.; Beck, B. H. *Tetrahedron Lett.* **1966**, 4523.
(25) Dalling, D. K.; Grant, D. M.; Johnson, L. F. *J. Am. Chem. Soc.* **1971**, *93*, 3678.
(26) Dale, J. *Top. Stereochem.* **1976**, *9*, 258.

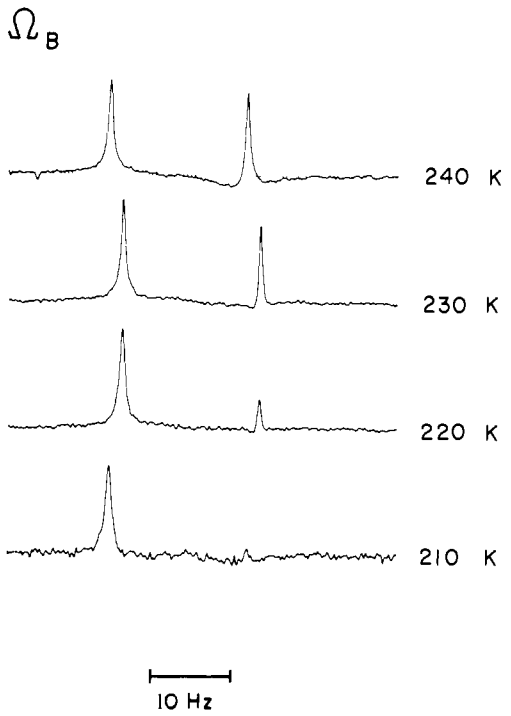

Figure 4. Cross sections extracted from phase-sensitive absorption-mode accordion spectra of *cis*-decalin, obtained at four different temperatures. Each cross section was taken at $\omega_2 = \Omega_B$ (chemical shift of carbons $C_4 + C_8$). The diagonal peaks (left) and cross-peaks (right) show characteristic line shapes in agreement with the simulations of Figure 2. The broader Lorentzian component (line width $2k + R_1$) is strongly temperature dependent. At low temperatures, the cross-peaks vanish because the antiphase components approach the same line width. The 10-Hz scale refers to the ω_m domain (equals 300 Hz in ω_1).

The absolute-value plot of the proton-decoupled carbon-13 accordion spectrum of *cis*-decalin, recorded at 240 K, is shown in Figure 3. Along the diagonal $\omega_1 = \omega_2$ (lower left to upper right corner) appear five peaks, which can be assigned to the sites $C_9 + C_{10}$, $C_4 + C_8$, $C_2 + C_6$, $C_1 + C_5$, and $C_3 + C_7$. Cross-peaks appear at the frequency coordinates of chemical shifts of interchanging sites. Note that both ω_1 and ω_2 axes in Figure 3 extend over 1500 Hz while the ω_m axis covers only 50 Hz because the ratio κ in eq 10 has been set to 30 in this experiment.

At first sight, Figure 3 closely resembles a normal two-dimensional exchange spectrum obtained with fixed mixing time t_m. In order to reveal the specific properties of the accordion spectrum, cross sections of the phase-sensitive spectrum must be inspected. For simplicity, we shall discuss the exchange between $C_1 + C_5$ (henceforth "site A") and $C_4 + C_8$ ("site B").

Figure 4 shows cross sections at $\omega_2 = \Omega_B$ extracted from four accordion spectra taken at four different temperatures (the top trace is extracted from the same data as Figure 3). To the left of each trace in Figure 4, at $\omega_1 = \Omega_B$, appears a diagonal peak with line shape $S_{BB}(\omega_m)$ while the right-hand peaks ($\omega_1 = \Omega_A$) are of the type $S_{AB}(\omega_m)$. The line shapes are in agreement with eq 11 and 12. It can be appreciated from the top trace in Figure 4 that both peaks have a positive, narrow component and a broad pedestal which is positive for the diagonal peak and negative for the cross-peak on the right. Cross sections through the same spectra at $\omega_2 = \Omega_A$ have a very similar appearance but for the fact that diagonal peaks and cross-peaks appear interchanged. Various procedures for analysis of these line shapes in terms of exchange rate constants will be treated in the next section.

V. Analysis of Accordion Line Shapes

We should like to propose three distinct strategies for the line-shape analysis in 2-D accordion spectra: (a) direct line-shape analysis, (b) reverse Fourier transformation, and (c) normal mode analysis by linear combination of cross sections. The choice of one of these methods will depend on the particular application.

(a) Direct Line-Shape Analysis. The ω_m line shapes of accordion spectra invariably consist of superpositions of Lorentzian lines with a common central frequency but with different widths and intensities. For the two-site case, discussed in the previous two sections, each line consists of just two Lorentzians, given by eq 11 and 12. In multiple-site systems (cf. section VI), the number of Lorentzians equals the number p of possible sites. Clearly, a least-squares procedure can be applied to extract the rate parameters involved. In some cases, the line shapes of the diagonal peaks cannot be relied upon because of overlapping signals along the diagonal ridge. It is then advisable to restrict the least-squares fitting procedure to the cross-peaks alone.

(b) Reverse Fourier Transformation. In many situations, the decay of the diagonal peaks and the buildup of the cross-peaks may be more revealing in the t_m time domain than in the ω_m frequency domain. This is particularly true for complex exchange networks such as commonly occur in transient Overhauser effects. In a linear system of the type $A \rightleftharpoons B \rightleftharpoons C$, the magnetization transfer from A to C is a second-order process. This can be immediately recognized in the t_m time domain, where the mixing function $a_{AC}(t_m)$ has a vanishing time derivative at $t_m = 0$ (in contrast to first-order processes). In general, as described in a separate communication,[27] it is possible to extract a signal $S(\omega_m)$ from an accordion spectrum and retrieve the corresponding time-domain mixing function $a(t_m)$ by means of a reverse Fourier transformation. To this effect, a cross section taken from the accordion spectrum is multiplied by a window function and subjected to a Fourier transformation. The envelope of the resulting signal is obtained by taking the absolute value in the time domain.[27]

(c) Linear Combinations of Cross Sections: Normal Mode Analysis. In systems where the diagonal peaks can be properly resolved, it is possible to exploit the complementary information contents of diagonal and cross-peaks. It is evident in the simple two-site exchange case shown in Figure 3 that cross sections taken parallel to ω_1 at $\omega_2 = \Omega_A$ and $\omega_2 = \Omega_B$ each have one diagonal peak and one cross-peak, which are necessarily aligned in the ω_1 dimension. It is therefore easy to take linear combinations of two cross sections:

$$S(\omega_1) = c_A S(\omega_1, \omega_2 = \Omega_A) + c_B S(\omega_1, \omega_2 = \Omega_B) \quad (13)$$

Such linear combinations amount to admixtures of diagonal-peak and cross-peak line shapes. At $\omega_1 = \Omega_A$, one obtains a line shape described by

$$S(\omega_m) = c_A S_{AA}(\omega_m) + c_B S_{AB}(\omega_m) \quad (14)$$

while at $\omega_1 = \Omega_B$ one obtains

$$S(\omega_m) = c_A S_{BA}(\omega_m) + c_B S_{BB}(\omega_m) \quad (15)$$

The meaning of these linear combinations is obvious by considering eq 11 and 12. The sum of two cross sections ($c_A = c_B = 1$) yields

$$S^{\Sigma}(\omega_m) = \frac{R_1}{R_1^2 + \omega_m^2} \quad (16)$$

while the difference ($c_A = 1$, $c_B = -1$) yields

$$S^{\Delta}(\omega_m) = \pm\frac{2k + R_1}{(2k + R_1)^2 + \omega_m^2} \quad (17)$$

Note that both linear combinations represent pure Lorentzians. The line width of $S^{\Sigma}(\omega_m)$ depends on R_1 only and is not affected by chemical exchange. This property stems from a conservation law: the exchange process neither creates nor destroys polarization but merely carries signal intensity from the diagonal peak to the cross-peak. Thus the sum of the two signals is damped only by longitudinal relaxation. The full line width $\Delta\nu_m^{\Sigma}$ at half-height of $S^{\Sigma}(\omega_m)$ provides a direct measure of the spin–lattice relaxation rate. An experimental example of such a linear combination (*cis*-decalin at 220 K) is shown in Figure 5. Note that both peaks

(27) Bodenhausen, G.; Ernst, R. R. *J. Magn. Reson.* **1981**, *45*, 367.

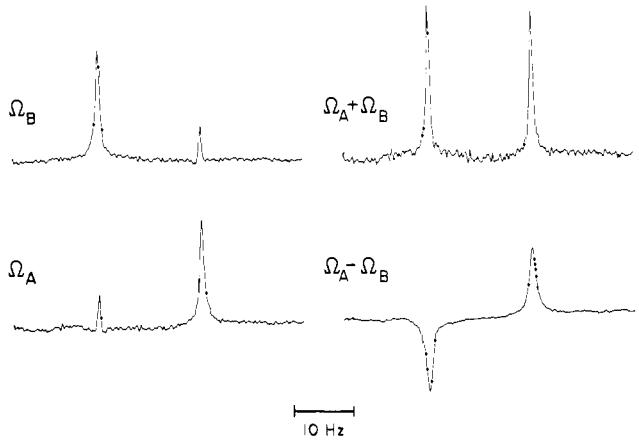

Figure 5. Left: Two cross sections through a phase-sensitive accordion spectrum of *cis*-decalin, recorded at 220 K, corresponding to $\omega_2 = \Omega_B$ (shift of carbons $C_4 + C_8$) and $\omega_2 = \Omega_A$ (shift of $C_1 + C_5$). Right: The sum of the two cross sections ($\Omega_A + \Omega_B$) yields two equal Lorentzian peaks with a width determined by the spin–lattice relaxation rate R_1. The difference ($\Omega_A - \Omega_B$) shows two broader peaks (width $2k + R_1$) with opposite phases. In this symmetrical two-site case, these linear combinations correspond to normal modes of the dynamic process.

Table I

temp, K	rate k, s^{-1}
240	13
230	4
220	0.9
210	0.2

in the sum $S^{\Sigma} = S(\omega_1, \omega_2 = \Omega_A) + S(\omega_1, \omega_2 = \Omega_B)$ have the same amplitude.

The effect of chemical exchange can be observed in the difference $S^{\Delta}(\omega_m)$ of two cross sections. Equation 17 describes a simple, broad Lorentzian with a full width at half-height $\Delta\nu_m^{\Delta} = (2k + R_1)/\pi$. As can be appreciated in Figure 5, the difference $S^{\Delta} = S(\omega_1, \omega_2 = \Omega_A) - S(\omega_1, \omega_2 = \Omega_B)$ features two peaks with the same line shapes but opposite intensities. The vanishing integral of the difference spectrum expresses the fact that the migration from A to B exactly cancels the reverse motion from B to A (microscopic reversibility in the dynamic equilibrium). The exchange rate k is readily obtained by subtracting the line widths in eq 16 and 17:

$$k = (\pi/2)(\Delta\nu_m^{\Delta} - \Delta\nu_m^{\Sigma}) \tag{18}$$

By measuring the difference in this manner, line-width contributions arising from T_2^* decay in the evolution time (see comments to eq 11 and 12) are canceled. Thus the exchange rate can be easily measured in accordion spectra without need for least-squares fitting or other kind of demanding data reduction.

Linear combinations of cross sections in two-dimensional spectra have been proposed elsewhere[28] in a different context, where coherence transfer among coupled spins was under investigation. In both cases, linear combinations have the additional advantage that much of the so-called t_1 noise may be cancelled to enhance the accuracy of the measurement.

Further experimental examples of linear combinations are shown in Figure 6. At all temperatures, the sums $S^{\Sigma}(\omega_m)$ show essentially the same line shapes, since the relaxation rate R_1 is not particularly sensitive to temperature. The differences $S^{\Delta}(\omega_m)$ in Figure 6, however, show the expected variation of the line width $\Delta\nu_m^{\Delta} = (2k + R_1)/\pi$ with temperature. By comparison of the line widths in the left and right halves of Figure 6, the exchange rates shown in Table I can be measured directly.

A simple Eyring plot, $-R \ln [k(1/\kappa_r)(h/k_B T)] = \Delta H^{\ddagger} (1/T) - \Delta S^{\ddagger}$, with the transmission factor $\kappa_r = 0.5$, as discussed by Dalling et al.,[25] yields $\Delta H^{\ddagger} = 58 \pm 3$ kJ mol^{-1} and $\Delta S^{\ddagger} = -26$ $\pm$ 30 J mol^{-1} K^{-1}, in fair agreement with earlier results[25] based on a much wider temperature range ($\Delta H^{\ddagger} = 56.9 \pm 2.9$ kJ mol^{-1} and $\Delta S^{\ddagger} = 15 \pm 12$ J mol^{-1} K^{-1}).

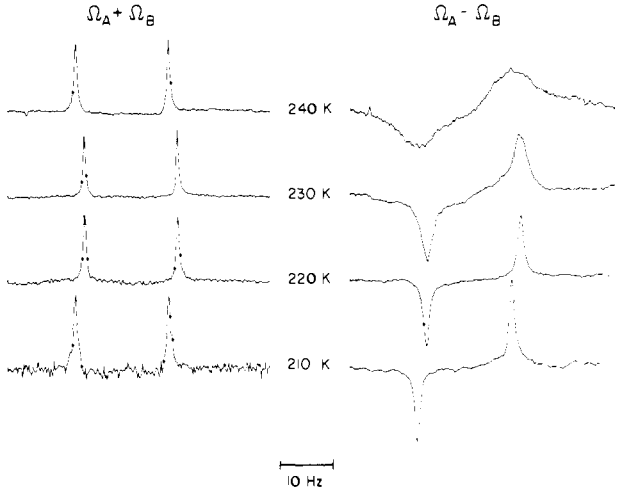

Figure 6. Linear combinations of cross sections taken from accordion spectra at four different temperatures. The sums $\Omega_A + \Omega_B$ (left) show essentially temperature-independent line widths determined by R_1. The differences $\Omega_A - \Omega_B$ show line widths $2k + R_1$. Comparison of the line widths left and right yields a straightforward measure of the temperature dependence of the exchange rate k.

The spectra in Figure 6 may be seen as a four-dimensional NMR experiment, since pseudo-3-D spectra have been obtained as a function of temperature. The entire series has been completed within 10 h of experimental time (Bruker CXP 300, 10-mm broad-band probe, ca. 70% *cis*-decalin in dioxane-d_8).

VI. Complex Exchange Networks

The accordion experiment can be used to investigate arbitrarily complex exchange networks. The principles, explained for a two-site system, remain the same. However, the evaluation of the data and the computation of the exchange rate constants become necessarily more involved.

The time evolution of the z magnetization in a p-site exchange network is determined by a set of p-coupled differential equations[16]

$$\mathbf{M}(t_m) = -(\Xi + \mathbf{R})\Delta\mathbf{M}(t_m) \tag{19}$$

where $\Delta\mathbf{M}(t_m) = (\mathbf{M}(t_m) - \mathbf{M}_0)$ is a p-dimensional vector of the deviations from thermal equilibrium of the longitudinal magnetizations M_i belonging to p sites; Ξ is the exchange matrix and $\mathbf{R}$ the (diagonal) relaxation matrix. The solution of the master equation (eq 19) is conveniently expressed in terms of the diagonal dynamic matrix $\mathbf{D}$.

$$\mathbf{D} = \mathbf{T}^{-1}(\Xi + \mathbf{R})\mathbf{T} \tag{20}$$

The diagonalizing transformation matrix $\mathbf{T}$ can be derived by standard procedures. The time dependence of the p sites is then given by

$$\Delta\mathbf{M}(t_m) = \mathbf{T} \exp(-\mathbf{D}t_m)\mathbf{T}^{-1}\Delta\mathbf{M}(t_m = 0) \tag{21}$$

or alternatively in terms of normal modes

$$\Delta\mathbf{N}(t_m) = \exp(-\mathbf{D}t_m)\Delta\mathbf{N}(t_m = 0) \tag{22}$$

where the elements of the vector $\mathbf{N}$ are linear combinations of the elements of the magnetization vector $\mathbf{M}$:

$$\mathbf{N} = \mathbf{T}^{-1}\mathbf{M} \tag{23}$$

Because of the nature of the excitation, the initial conditions $\Delta\mathbf{M}(t_m = 0)$ of the time evolution have a particularly simple form in the accordion experiment. All peaks on a given row of the 2-D spectrum (i.e., with a common ω_1 frequency) share the same initial preparation. All peaks with $\omega_1 = \Omega_i$ have $\Delta M_i(t_m = 0) = -2M_{0i}$ and $\Delta M_j(t_m = 0) = 0$ for $j \neq i$. As a result, the t_m time dependence of all peaks in the two-dimensional accordion spectrum can be expressed in matrix notation:

(28) Bodenhausen, G.; Bolton, P. H. *J. Magn. Reson.* **1980**, *39*, 399.

$$\mathbf{a}(t_m) = \mathbf{T}\exp(-\mathbf{D}t_m)\mathbf{T}^{-1}\mathbf{M}_0^{\text{matrix}} \quad (24)$$

where the diagonal matrix $\mathbf{M}_0^{\text{matrix}}$ contains the same elements as the vector $\mathbf{M}_0$ of the equilibrium magnetizations $(\mathbf{M}_0^{\text{matrix}})_{ii} = (\mathbf{M}_0)_i$. The elements of **a** correspond to the mixing functions and represent peak amplitudes in two-dimensional frequency domain (e.g., $a_{ij} = a(\omega_1 = \Omega_i, \omega_2 = \Omega_j)$).

Equation 24 is a generalization of the specialized expressions 7 and 8. In the two-site case with equal populations and equal relaxation times, we have

$$\mathbf{T} = \begin{pmatrix} 1 & -1 \\ 1 & 1 \end{pmatrix}$$

$$\mathbf{D} = \begin{pmatrix} -R_1 & 0 \\ 0 & -(2k + R_1) \end{pmatrix}$$

$$\mathbf{M}^{\text{matrix}} = \begin{pmatrix} M_{0A} & 0 \\ 0 & M_{0B} \end{pmatrix}$$

where the equilibrium magnetizations M_{0A} and M_{0B} are equal. Equation 24 implies that each peak in a p-site accordion spectrum arises from a superposition of p exponential functions. The line-shape functions in the ω_m frequency domain must therefore consist of p Lorentzian components. For a peak connecting the chemical shifts of two sites i and j, one obtains

$$S_{ij}(\omega_m) = \sum_{q=1}^{p} T_{iq}T_{qj}^{-1}\frac{D_q}{D_q^2 + \omega_m^2}M_{0j} \quad (25)$$

These line shapes can be analyzed by the same procedures which have been described for the two-site case. Least-squares analysis, reverse Fourier transformation, or normal mode analysis may each have their advantages in specific situations. A more extensive discussion of multisite exchange will be given elsewhere.[29]

VII. Coupled Spin Systems

It has been assumed so far that the systems under investigation consist only of isolated spins with $I = {}^1/_2$. Applications of accordion spectroscopy to coupled spin systems may lead to complications which are closely related to those encountered in standard 2-D exchange methods.[23] Ideally, only longitudinal (incoherent) magnetization should evolve in the t_m interval. In practice, however, the second 90° pulse may excite multiple-quantum coherence which precesses in t_m, leading to spurious modulations which transform into so-called J cross-peaks. Higher orders of multiple-quantum interference can be suppressed by appropriate phase cycling,[30] but zero-quantum interference cannot easily be separated from longitudinal magnetization. These undesirable signal contributions may persist for long t_m intervals (since they are not sensitive to field inhomogeneity) and thus generate spurious narrow peaks in accordion spectra.

Macura et al.[31] have recently proposed a 2-D exchange technique to identify multiple-quantum interference. Like in the accordion experiment, the mixing time is incremented along with t_1:

$$t_m = t_m^0 + \kappa t_1 \quad (26)$$

In contrast to the accordion experiment, κ is small, and t_m remains essentially constant on the time scale of exchange processes. Multiple- and zero-quantum interferences are, however, modulated by the variation of t_m, resulting in displacements of multiple-quantum signals in the ω_1 direction. A similar effect may be achieved unwittingly in the accordion experiment. For suppression of zero-quantum effects, it is possible to introduce a 180° refocusing pulse in the t_m delay and vary its position randomly between subsequent transients of the time-averaging process.[23] With these precautions, it appears that applications to coupled spin systems are quite feasible. It must be kept in mind, however, that multiplets due to scalar coupling may be ill-resolved, particularly in large molecules, leading to overlapping accordion line shapes.

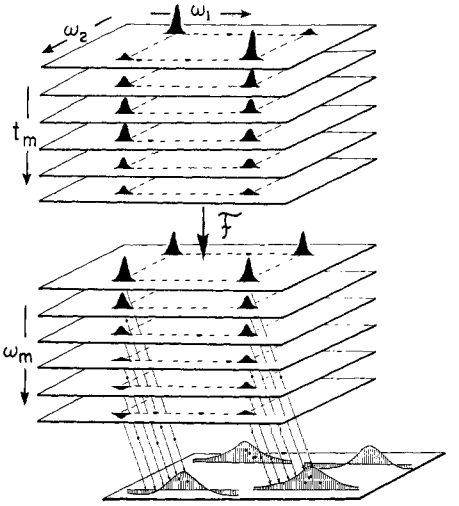

Figure 7. Schematic representation of the reduction of three- to two-dimensional spectroscopy achieved in the accordion method. Top: A true 3-D exchange spectrum can be visualized as a stack of 2-D spectra $S(\omega_1,\omega_2)$ recorded with systematic increments of t_m. The diagonal peaks decay monotonically, while cross-peaks first increase and later decay as a function of t_m. Middle: By Fourier transformation with respect to t_m, a three-dimensional frequency domain $S(\omega_1,\omega_m,\omega_2)$ is obtained. Provided the spectrum is well resolved in ω_1, a skew projection (bottom) can be made without entailing any loss of information. The same spectrum can be obtained directly and much more efficiently by the accordion method, where t_m and t_1 are incremented together.

VIII. Discussion and Conclusion

The approach outlined in this paper appears to provide a versatile tool for studying chemical exchange and cross-relaxation. The reduction of the dimension from three to two opens the way to studies which would normally present prohibitive demands on experimental time. At this point, it appears appropriate to discuss the connection between the accordion experiment and true three-dimensional spectroscopy. The latter may be visualized as a stack of 2-D spectra $S(\omega_1,t_m,\omega_2)$, shown schematically in Figure 7 (top). An additional Fourier transformation with respect to t_m yields a true 3-D spectrum $S(\omega_1,\omega_m,\omega_2)$ (Figure 7, middle) where the line shapes carrying the exchange information extend along a separate frequency axis ω_m. In the accordion experiment, this ω_m domain is projected along a skew line onto the ω_1 axis, the slope $\Delta\omega_m/\Delta\omega_1$ of the skew projection being determined by κ. This procedure, shown schematically in Figure 7 (bottom), is reminiscent of the reduction of dimension inherent in some NMR imaging techniques.[32,33] Clearly, the skew projection of the accordion experiment need not entail any loss of information, provided the chemical shifts in the ω_1 domain are sufficiently dispersed to accommodate the line shapes without extensive overlap. There may be some interference in crowded spectra or in systems with ill-resolved scalar couplings. Fortunately, experience has shown that a great deal of dynamic information can be obtained even in situations which depart from ideal conditions.

Acknowledgment. We are grateful to Dr. S. Macura for helpful discussions and for software modifications to the CXP program required for phase-sensitive 2-D FT. Janos Deli provided valuable assistance with the experiments, and I. Müller kindly prepared the manuscript. This research has been supported in part by the Swiss National Science Foundation.

Registry No. *cis*-Decalin, 493-01-6.

(29) Bodenhausen, G.; Ernst, R. R., in preparation.
(30) Wokaun, A.; Ernst, R. R. *Chem. Phys. Lett.* **1977**, *52*, 407.
(31) Macura, S.; Wüthrich, K.; Ernst, R. R. *J. Magn. Reson.*, in press.
(32) Mansfield, P.; Maudsley, A. A. *J. Phys. C* **1976**, *9*, L409; Mansfield, P. *Ibid.* **1977**, *10*, L55.
(33) Brunner, P.; Ernst, R. R. *J. Magn. Reson.* **1979**, *33*, 83.